JMES The International Journal of
Mechanical Engineering and Sciences
https://iptek.its.ac.id/index.php/jmes
e-ISSN 2580-7471

Influence of Front and Rear Wings on Aerodynamic Forces in a Student Formula Car

Dedy Zulhidayat Noor[1*], Heru Mirmanto[1], Arino Anzip[1], Herman Sasongko[2]
[1]Department of Industrial Mechanical Engineering, ITS, Sukolilo Surabaya 60111, Indonesia
[2]Department of Mechanical Engineering, ITS, Sukolilo Surabaya 60111, Indonesia

Received: 27 July 2024, Revised: 30 September 2024, Accepted: 30 September 2024

Abstract

Aerodynamic forces affect the stability of a car when moving, especially when turning. This study conducted a CFD analysis of the influence of wings on the student formula car when turning. The addition of front and rear wings to the formula car increases drag, downforce, and side forces. Except for an airplane that is landing, large drag forces are always avoided, as well as side forces that can interfere with vehicle stability. Compared to cars without wings, in cars with front and rear wings, increasing the cornering speed from 40 km/h to 60 km/h increases the drag from 8.046% to 114.43%, while downforce increases from 222.85% to 231.52%. Interestingly, in contrast to the drag and downforce, the increase in the lateral force coefficient tended to decrease continuously, from 26.74% to 10.25%, as the cornering speed increased. The increase in downforce or negative lift in this formula car is more dominant and significant than that in the others, and it is very beneficial in increasing wheel grip and traction on the car's stability when turning.

Keywords: Formula car, wing, cornering, drag, downforce, side force, stability

1. Introduction

Drag and lift are aerodynamic forces that arise when a vehicle moves. Drag is desired to be small for freedom of movement and reduced energy consumption but is expected to be high during braking. The use of flaps on aircraft wings is one example. In an airplane, positive lift helps overcome the force of gravity. Meanwhile, negative lift, also known as downforce, increases the stability of land vehicles when moving on the ground. Downforce must ensure better stability and safety for a racing vehicle moving at high speed. One technique for increasing downforce is to create a diffuser in the vehicle's underbody [1–4]. Another method to increase downforce is to place a spoiler on the body of a vehicle [5–7]. On the other hand, a wing with an airfoil cross-section provides a higher increase in downforce than a spoiler. A spoiler has airflow on one side and a wing on both sides.

The placement of the front wing produces 30% of the overall downforce on a Formula 1 car; likewise, the angle of attack and the distance between the wing and the car affect aerodynamic forces [8]. Vehicle stability is supported by the grip of the wheels on the ground. Statistically, 20% of the grip is obtained from the weight of the vehicle itself, whereas 80% comes from the downforce generated by the rear wings [9]. Another study showed that adding a front or rear wing to a student formula car provides a balanced increase in downforce, namely 83% while using both together provides an increase of up to 91% [10]. When a vehicle moves on a curved track, the airflow structure across it becomes asymmetrical, creating a pressure difference between the inboard and outboard sides. This pressure difference produces side forces as the vehicle moves in a straight line with a crosswind.

For formula cars, maintaining stability when cornering is a critical issue. It is also done to examine the front wing's influence during cornering. To lessen turbulence, the cascade front wing is fitted with end plates at the tips of the wings. Nevertheless, the cascade wing's airflow behavior drastically alters when the vehicle turns. When an automobile is cornering, its yaw angle increases, which causes its drag and downforce to decrease inversely [11]. The previous study used an active rear wing to create more downforce and traction to prevent the car from slipping and rolling during cornering. In terms of stability, the use of wings increases cornering velocity by up to 16% [12]. Another study used a twisted rear wing to increase cornering velocity by up to 13% [13].

Studies of vehicle aerodynamic forces when turning are mostly focused on the use of front or rear wings. Based on our literature review, there is a lack of information regarding the simultaneous use of front and rear wings in terms of their influence on the aerodynamic forces during cornering. In this study, we simulated the influence of front and rear wings on the aerodynamic forces of a student formula car, especially downforce during corner-

*Corresponding author. Email: zulhidyat@its.ac.id

ing. Car dimensions, including width, length, height, and ground clearance, are adjusted to the rules of the SAE Australasian event, as well as operating conditions such as track curvature and speed [14].

2. Numerical Method

We used Ansys-Fluent to study the effect of using wings on the aerodynamic forces in the car student formula when turning. The study's shortcomings are that it was challenging to replicate in a computational analysis the actual operating circumstances for a turbulent flow. Our computational domain follows the previous research [15], as shown in Figure 1, where L is the length of the car. The boundary conditions for the inlet and outlet are velocity and pressure respectively, while the vehicle body and ground are no-slip walls. Simulations were carried out for steady conditions with k–ϵ Realizable as the turbulent model.

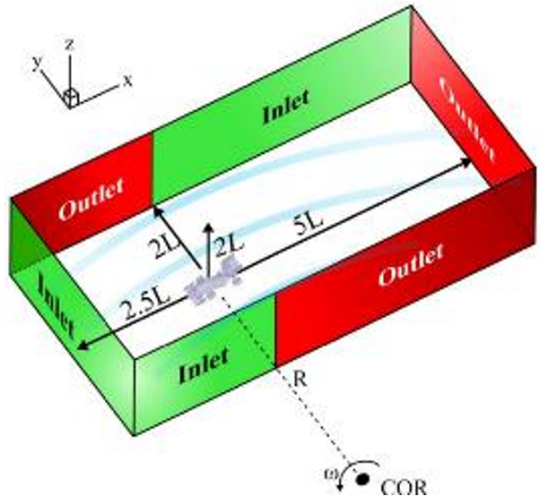

Figure 1. Computational domain and boundary conditions [14, 15]

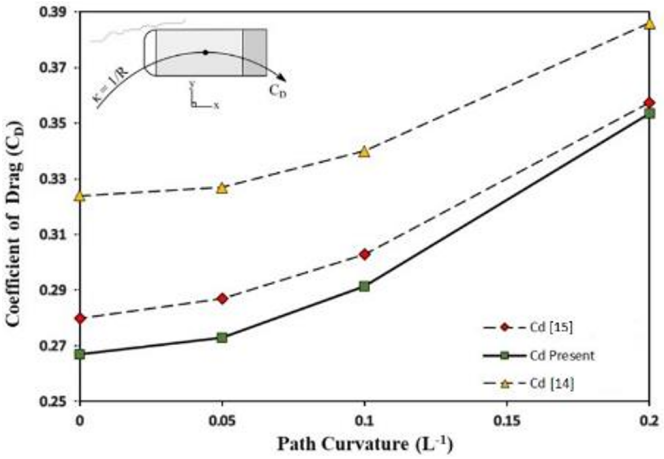

Figure 2. Coefficient of drag based on changes in radius curvature.

Before carrying out further research, we validated our numerical model with previous research [16]. Figure 2 shows the CD values at various radius curvatures for cornering motion. Qualitatively, there is conformity with the previous research, namely an increase in the drag coefficient that is directly proportional to the increase in the curvature of the vehicle path. Quantitatively, the big difference is in small-radius curvature with a value of around 3.5%. It shows a good agreement with the previous research.

The model we used in this study is shown in Figure 3. We chose NACA Eppler E-423 airfoil for the front and rear wings, and the wing geometries are shown in Figure 4.

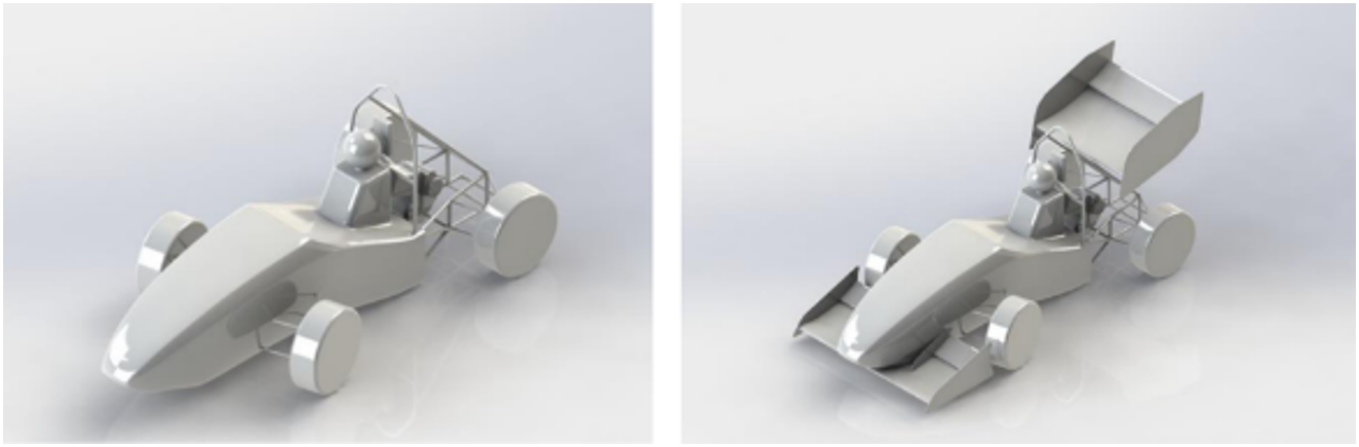

Figure 3. Simulation models.

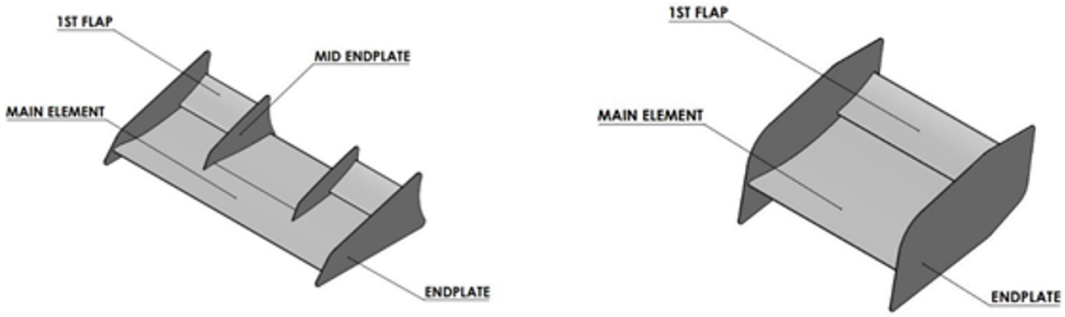

Figure 4. Geometry of font (left) and rear (right) wings.

Table 1. Grid Independency test

Mesh	Total Number of Cells	Quality		CD	FD (N)	CL	FL (N)
		Max. Skew.	Min. Orth				
A	2,767,563.00	0.89	0.15	0.09352	10.2	0.111906	12.21
B	3,814,522.00	0.84	0.15	0.09129	9.96	0.145554	15.88
C	4,456,995.00	0.72	0.28	0.0941	10.26	0.105343	11.49
D	6,042,492.00	0.76	0.25	0.09387	10.24	0.109421	11.93

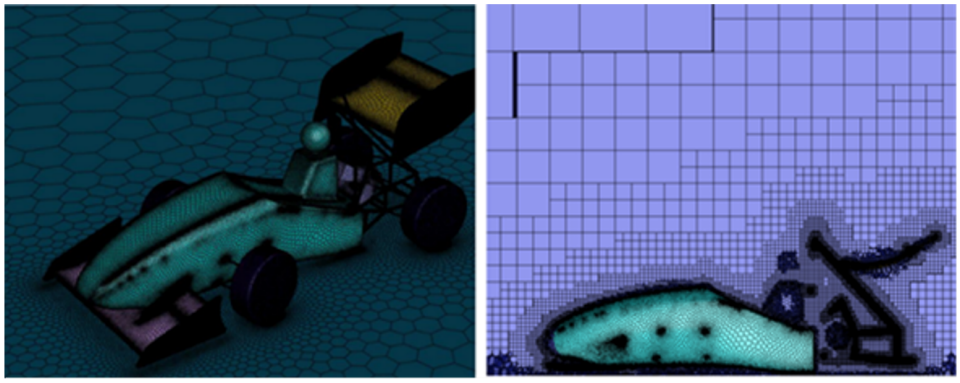

Figure 5. Mesh C with a total of 4,456,995,000 cells.

The grid independence test is carried out to determine the accuracy of the mesh pattern used. We perform a grid independence study by creating a variable for the number of cells in the mesh with the same boundary conditions. We use the values of drag coefficients as a comparison analysis between the chosen mesh. In this grid independence analysis, four mesh variations were created, namely mesh A, B, C, and D. The results of the grid independence analysis are shown in Table 1. CD, CL, FD, and FL are the analysis parameters for the four mesh variations. Mesh pattern D has the largest number of cells and high mesh quality. Furthermore, it needs more computational time for convergency. Mesh patterns A, B, and C do not have significant differences in the CD values compared to mesh D, except for mesh A and B in the CL parameter. Therefore, mesh C (Figure 5) is used in this research because the difference in parameter values is not significant compared to mesh D. It has high mesh quality, and the smaller number of cells makes it possible to get convergent results with a shorter time.

3. Results and Discussion

Figure 6 shows the pressure distribution on the surface of a vehicle without wings when turning. The difference in pressure distribution on the inboard and outboard surfaces of the vehicle is caused by changes in the structure, characteristics, and angle of the freestream flow toward the center point of the vehicle's turning radius. The red color contour plot indicates a higher-pressure distribution that appears in the inboard area, and a lower-pressure distribution appears in the outboard area of the vehicle. The difference in pressure on the inboard and outboard produces side forces that affect the yawing moment. The location that receives the highest pressure appears on the inboard surface areas of the body, driver, engine, frame, and tires which are the vehicle's stagnation points.

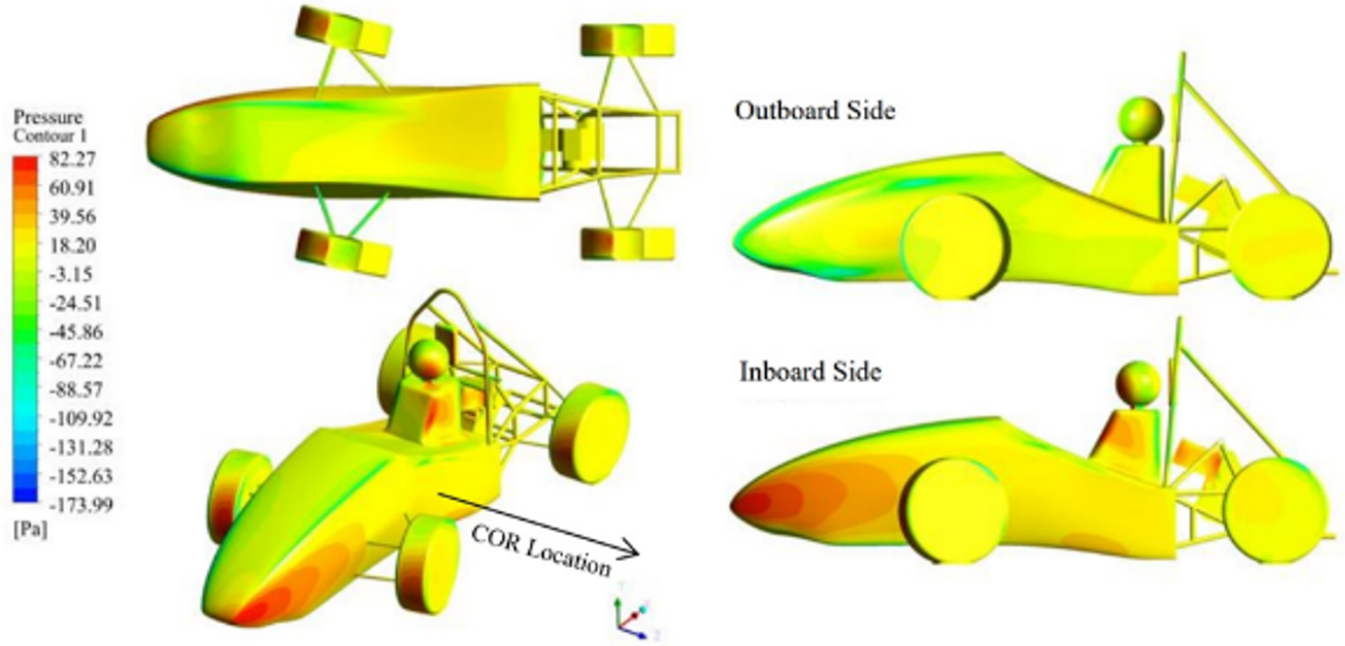

Figure 6. Pressure distribution on a car without wings.

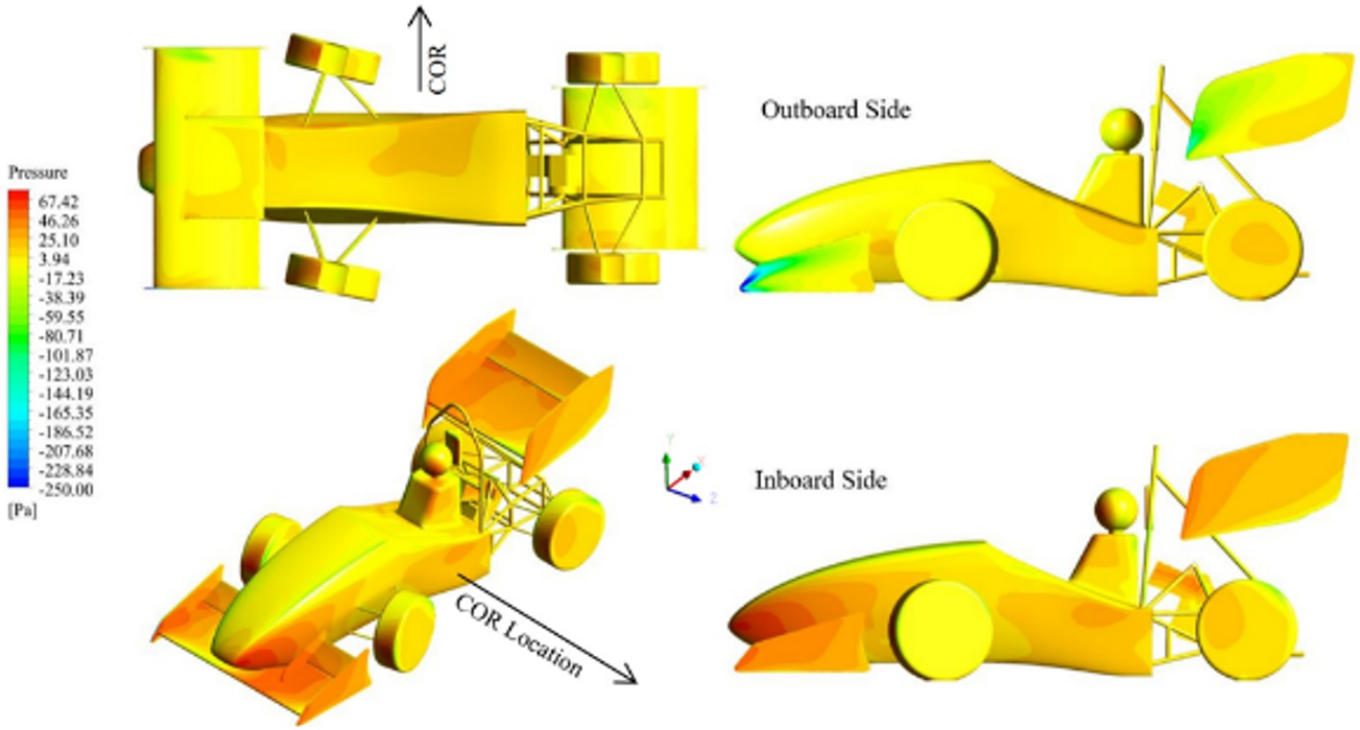

Figure 7. Pressure distribution on a car with wings.

Figure 7 shows the pressure distribution for a vehicle with the addition of wings. As in the case without wings, the areas that receive the highest pressure appear on the inboard surface area of the body, driver, engine, frame, and tires. The presence of a front wing increases the area that has a higher-pressure distribution compared to a car without it, but the maximum pressure obtained by the vehicle decreases by 70 Pa compared to the maximum pressure obtained by a vehicle without wings is 82.27 Pa.

Visualization of the flow when passing through all vehicle components when turning at a constant radius is shown in Figure 8. Air flow at a low speed is marked in

blue and air flow at a high speed is marked in red. The low-speed flow which is the wake area is located behind the driver, headrest, and vehicle engine. This wake area appears because the flow is separated at the vehicle components which are called separation points, so that there is a flow velocity gradient in this area and the flow profile will change to reverse flow which then develops into a wake area. Wake downstream is an area with low pressure, which increases the drag received by the car. Vortices produced due to pressure differences on the top and bottom surfaces of the wing flaps point towards the inboard side like streamlines, this proves that drag works following the curvature of the vehicle's path.

The addition of this aerodynamic device increases the area on the sides causing an increase in the aerodynamic side force acting on the vehicle. Because the pressure distribution on the inboard side is predominantly higher than on the outboard side, the side force is unfavorable because it works in the same direction as the vehicle's centrifugal force.

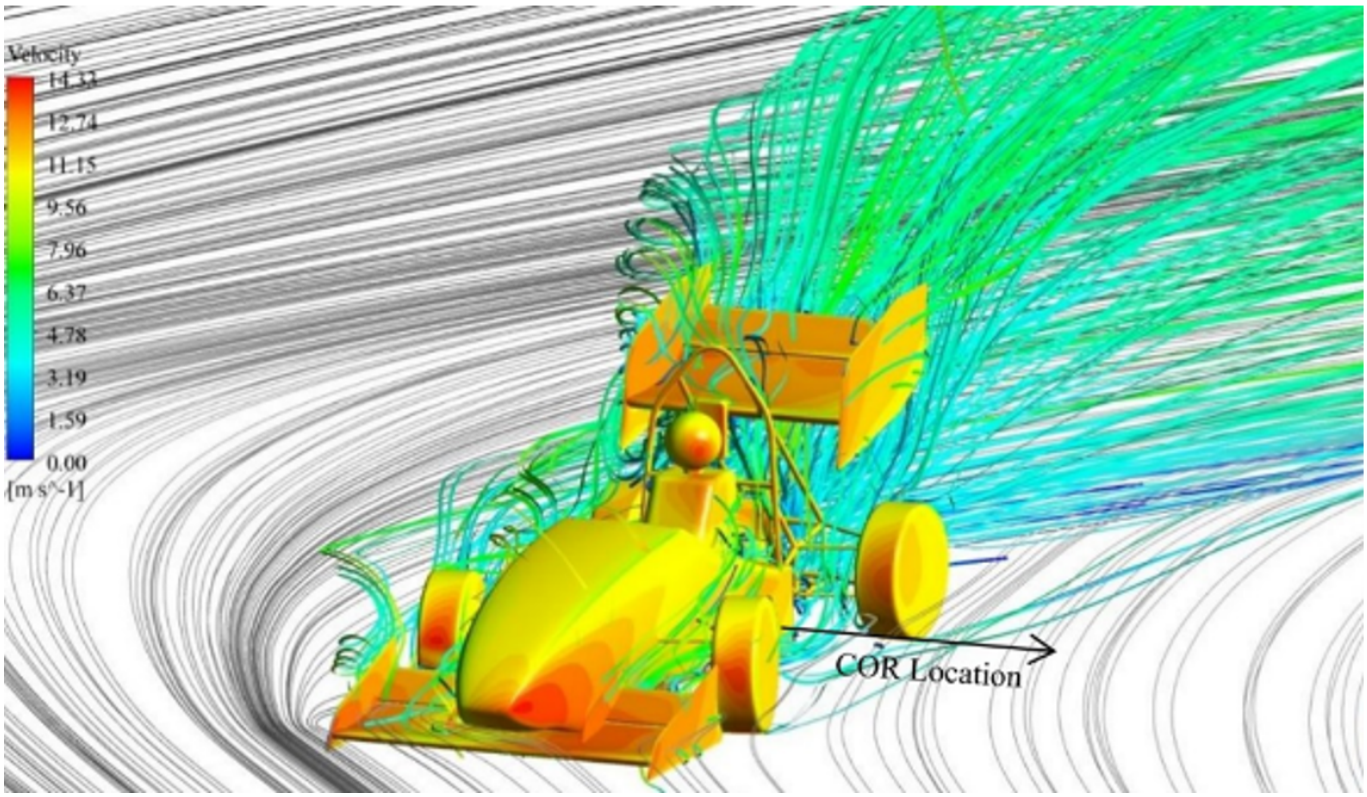

Figure 8. Velocity streamlines and body pressure contours.

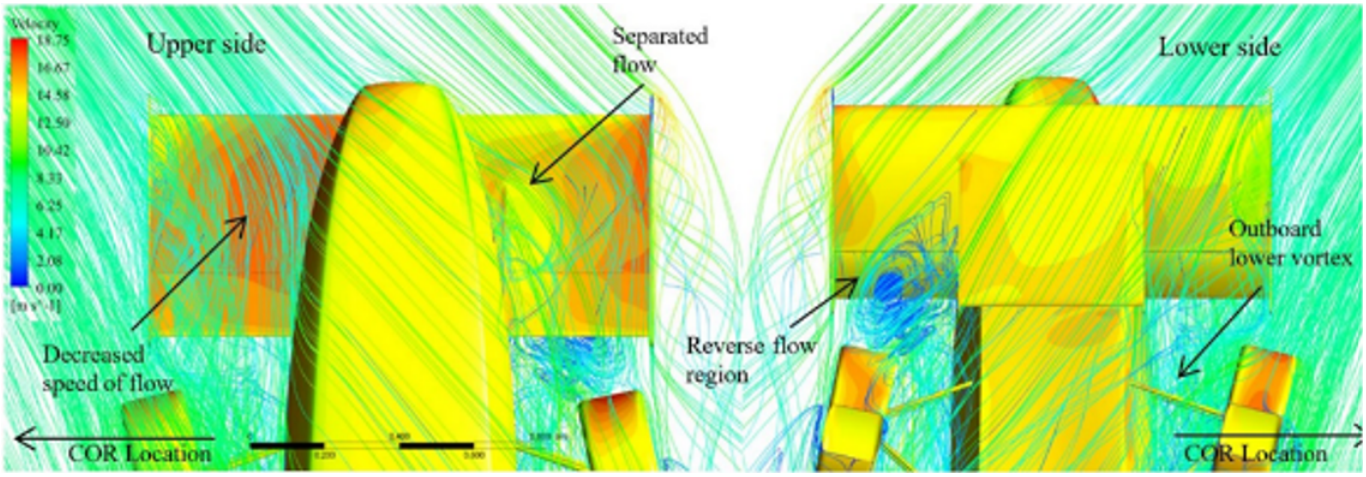

Figure 9. Pressure distribution on the front wing and the velocity streamlines around it.

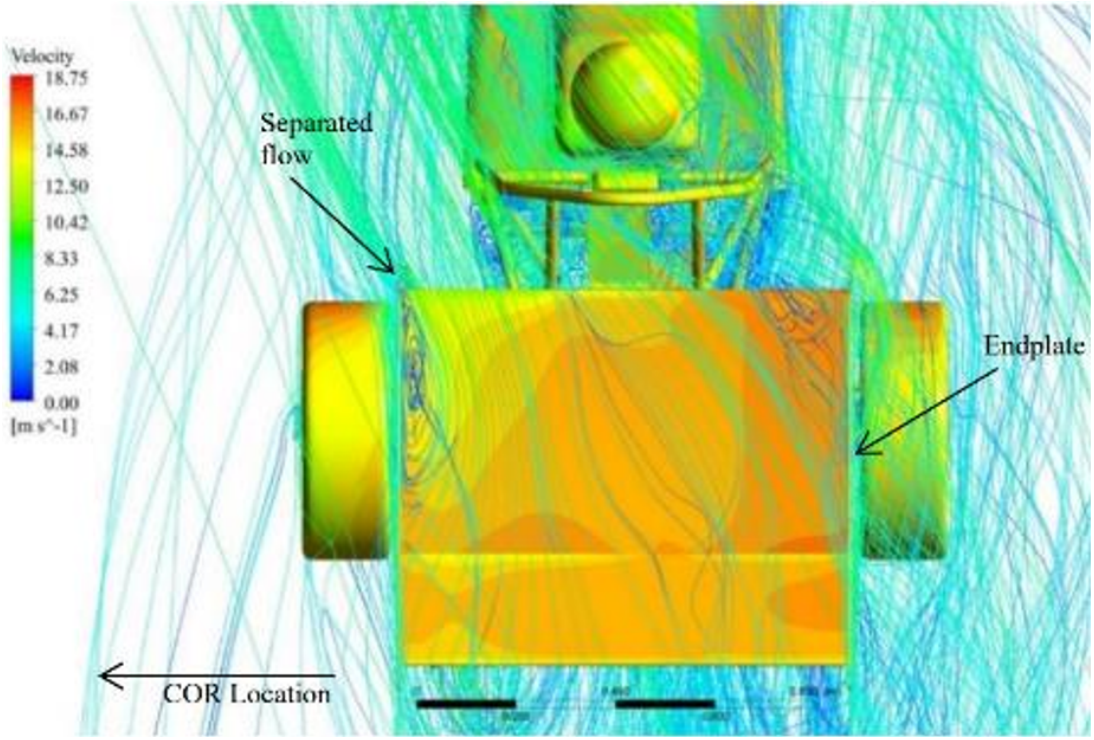

Figure 10. Pressure distribution on the rear wing and the velocity streamlines around it.

Figure 9 shows the pressure distribution on the upper and lower wings as well as the velocity streamlines around them. The pressure distribution on the upper wing is higher than on the lower part, resulting in beneficial downforce for the car. The flow intensity on the inboard side of the vehicle is more dominant than on the outboard side of the vehicle. This occurs due to the curvature of the flow direction and the flow passing through the separation point or area. In this case, the flow is separated by the nosecone component so that the intensity and momentum of the flow passing through the outboard side of the front wing decreases. This causes differences in pressure distribution on the upper surface of the front wing on the inboard and outboard sides. Air flows marked in blue indicate low-velocity flows. On the top surface of the front wing inboard side, there is a green streamline which then becomes light blue as shown by the arrow in the picture. This indicates a slowdown in flow velocity because it passes through the surface of the main flap which has an inverted airfoil profile and causes increased pressure in that area. The use of endplates on the front wing device has been proven to increase efficiency as shown in the picture above, the endplates can capture momentum and direct airflow towards the front wing main flap. The airflow separated by the nosecone component is also related to the formation of a regional backflow that appears at the bottom of the outboard side of the front wing.

Table 2. Drag coefficient (Cd) for different cornering velocities.

Variation		Coefficient Drag (CD)				
Car	Velocity (km/h)	Body	Frontwing	Rear wing	Total	Add (%)
FSN w/o wings	40	0.0887579	-	-	0.088758	
	45	0.0907393	-	-	0.090739	
	50	0.0871183	-	-	0.087118	
	55	0.0804227	-	-	0.080423	
	60	0.0805696	-	-	0.08057	
FSN with wings	40	0.089	0.0281783	0.0476847	0.1651	86.04%
	45	0.091	0.0282582	0.0490182	0.1687	85.93%
	50	0.084	0.0307587	0.0545986	0.1696	94.64%
	55	0.086	0.0314611	0.0544892	0.1718	113.66%
	60	0.086	0.0322209	0.0541567	0.1728	114.43%

Table 3. Downforce/negative lift coefficient (Cl) for different cornering velocities.

Variation		Coefficient Lift (CL)				
Car	Velocity (km/h)	Body	Frontwing	Rear wing	Total	Add (%)
FSN w/o wings	40	0.114	-	-	0.114	-
	45	0.139	-	-	0.139	-
	50	0.137	-	-	0.137	-
	55	0.144	-	-	0.144	-
	60	0.143	-	-	0.143	-
FSN with wings	40	0.186	-0.178	-0.149	-0.141	222.85%
	45	0.189	-0.181	-0.155	-0.147	205.60%
	50	0.187	-0.189	-0.174	-0.176	228.94%
	55	0.178	-0.19	-0.178	-0.19	232.31%
	60	0.178	-0.19	-0.177	-0.189	231.52%

Table 4. Side force coefficient (Cs) for different cornering velocities

Variation		Side coefficient (CS)				
Car	Velocity (km/h)	Body	Front wing	Rear wing	Total	Add (%)
FSN w/o wings	40	0.333	-	-	-0.333	
	45	0.34	-	-	-0.34	
	50	0.331	-	-	-0.331	
	55	0.324	-	-	-0.324	
	60	0.336	-	-	-0.336	
FSN with wings	40	0.146	-0.115	-0.161	-0.422	26.74%
	45	0.141	-0.113	-0.159	-0.413	21.63%
	50	0.158	-0.097	-0.116	-0.371	12.37%
	55	0.163	-0.098	-0.12	-0.382	17.76%
	60	0.154	-0.098	-0.119	-0.371	10.25%

Figure 10 shows the pressure distribution on the rear wing surface and the surrounding flow field. High-pressure distribution on the upper surface produces downforce on the rear wing. Flow separation occurs on the inboard side which forms a backflow on the main flap upper surface. The presence of the endplates directs the flow back parallel to the original direction of the rear wing, thus preventing the enlargement of the backflow area which erodes flow momentum. This phenomenon is known as bubble separation, where a flow that loses momentum and detaches from the solid body receives energy from the fluid layer above it so that it attaches to the surface. The wake found at the beginning of the main flap on the outboard side comes from the flow separation that forms behind the driver. Apart from directing the flow following the vehicle's path, the endplates also prevent the high-pressure airflow on the upper surface from rolling into the low-pressure area below which causes increased drag.

Table 2 - 4 show the drag, lift and side force coefficients at various turning speeds. The presence of front and rear wings produces variations in drag, downforce, and side force values. The values of these three forces increase with the addition of wings. The rear wing provides more drag and side force than the front wing. The drag value continues to be greater with increasing speed. Interestingly, on the other side, the opposite happens with side force. The side force value decreases with increasing speed when turning.

In terms of resulting downforce, the front wing has more contribution than the rear one. For a moving vehicle, increased drag is detrimental. Likewise, increasing side force is not beneficial when turning because it increases the centrifugal force that tends to push it out of its path. However, the percentage increase in downforce is more significant, providing better grip on the ground and stability when the vehicle moves on a curved track. Cars without wings have a positive lift force that only relies on its weight to maintain stability. On the other hand, apart from producing downforce on the wing, the body of the car also gets it so that the presence of wings increases the total downforce more than twice.

4. Conclusions

Based on the simulation and analysis results, several points can be concluded as follows:

1. Front and rear wings on the Formula car increase drag, downforce, and side force compared to with-

out wings. The percentage increase in downforce is more dominant than drag and side force.

2. The more the pressure difference between the upper and lower surfaces of the wings, the greater the downforce. However, this is also accompanied by an increase in drag.

3. When turning, the streamlines are asymmetrical, creating a pressure difference on the inboard and outboard sides and producing side force in the same direction as the centrifugal force.

4. The coefficient of side force is relatively constant on the car without wings and tends to decrease on the car with wings as cornering velocities increase.

5. Acknowledgments

We thank our university for providing a computing facility.

References

[1] R. Dominy, "Aerodynamics of grand prix cars," *Proceedings of the Institution of Mechanical Engineers, Part D: Journal of Automobile Engineering*, vol. 206, no. 4, pp. 267–274, 1992.

[2] D. L. Garcia and J. Katz, "Trapped vortex in ground effect," *AIAA journal*, vol. 41, no. 4, pp. 674–678, 2003.

[3] A. Singh, A. Jain, and A. Sharma, "Designing a 3-d model of bodywork of a vehicle with low coefficient of drag and high downforce," *Materials Today: Proceedings*, vol. 28, pp. 2197–2204, 2020.

[4] F. F. Buscariolo, G. R. Assi, and S. J. Sherwin, "Computational study on an ahmed body equipped with simplified underbody diffuser," *Journal of Wind Engineering and Industrial Aerodynamics*, vol. 209, p. 104411, 2021.

[5] K. Singh, H. Bahri, H. Singh, and J. Singh, "A review of "performance analysis and optimization of car air spoilers"," in *IOP Conference Series: Materials Science and Engineering*, vol. 691, p. 012056, IOP Publishing, 2019.

[6] Z. Deng, S. Yu, W. Gao, Q. Yi, and W. Yu, "Review of effects the rear spoiler aerodynamic analysis on ground vehicle performance," in *Journal of Physics: Conference Series*, vol. 1600, p. 012027, IOP Publishing, 2020.

[7] M. A. J. Selvam, M. R. Kumar, S. Padmanabhan, K. H. S. Subramanyam, and M. N. Reddy, "Analyzing the downforce generated by rear spoiler of hatchback vehicle and creating an aeromapp using cfd analysis," *Materials Today: Proceedings*, vol. 92, pp. 48–55, 2023.

[8] S. Durrer, "Aerodynamics of race car wings: A cfd study," 2016.

[9] T. Zhou and Z. Zeng, "Optimal aerodynamic design for formula sae car using curved wings," *Chongqing Daxue Xuebao/Journal of Chongqing University*, vol. 40, pp. 40–52, 10 2017.

[10] A. Y. E. Nugraha, "Numerical simulation of the effect of adding a front wing and rear wing on the aerodynamic performance of the its nogogeni formula student car," 2021.

[11] A. T. Raheem, A. Sapit, and A. N. Mohammed, "Aerodynamics of a formula one car front cascade wing during cornering," *Journal of Advanced Research in Fluid Mechanics and Thermal Sciences*, vol. 53, no. 1, pp. 53–60, 2019.

[12] V. Chiplunkar, R. Gujar, A. Adiverekar, R. Kulkarni, and A. Thonge, "Computational fluid dynamics analysis for an active rear-wing design to improve cornering speed for a high-performance car," *Materials Today: Proceedings*, vol. 77, pp. 887–896, 2023.

[13] J. R. Piechna, K. Kurec, J. Broniszewski, M. Remer, A. Piechna, K. Kamieniecki, and P. Bibik, "Influence of the car movable aerodynamic elements on fast road car cornering," *Energies*, vol. 15, no. 3, p. 689, 2022.

[14] "https://www.saea.com.au/formula-sae-a,"

[15] J. Keogh, T. Barber, S. Diasinos, and G. Doig, "Techniques for aerodynamic analysis of cornering vehicles," *SAE Technical Papers*, vol. 2015, 03 2015.

[16] J. Keogh, T. Barber, S. Diasinos, and D. Graham, "The aerodynamic effects on a cornering ahmed body," *Journal of Wind Engineering and Industrial Aerodynamics*, vol. 154, pp. 34–46, 07 2016.